Ferromagnetic resonance force microscopy studies of arrays of micron size permalloy dots

T. Mewes,[1,2,*] J. Kim,[1] D. V. Pelekhov,[1] G. N. Kakazei,[1,3] P. E. Wigen,[1] S. Batra,[4] and P. C. Hammel[1,†]
[1]*Department of Physics, Ohio State University, 191 West Woodruff Avenue, Columbus, Ohio 43210, USA*
[2]*Center for Materials for Information Technology and Department of Physics & Astronomy,University of Alabama, Box 870209, Tuscaloosa, Alabama 35487, USA*
[3]*Institute of Magnetism National Academy of Sciences of Ukraine, 36b Vernadskogo Boulevard, 03142 Kiev, Ukraine*
[4]*Seagate Research, 1251 Waterfront Place, Pittsburgh, Pennsylvania 15222, USA*
(Received 7 June 2006; revised manuscript received 16 August 2006; published 25 October 2006)

The dynamic magnetic properties of micron-sized permalloy disks have been investigated using magnetic resonance force microscopy. From local spectroscopy data, information about the global sample properties is obtained. The experimental results are in good agreement with theoretical predictions, which account for magnetostatic modes with quantized in-plane wave vector. Ferromagnetic resonance spectral features due to the permalloy dots in close proximity to the micromagnetic probe tip provide two-dimensional images of the sample.

DOI: 10.1103/PhysRevB.74.144424 PACS number(s): 75.30.Ds, 75.75.+a, 07.79.Pk, 76.50.+g

I. INTRODUCTION

Since magnetic resonance force microscopy (MRFM) was first proposed by Sidles in 1991,[1] it has evolved into a three-dimensional magnetic imaging technique with excellent sensitivity and spatial resolution. Recently, Rugar *et al.* reported the detection of a single electron spin in silicon dioxide using MRFM.[2] Besides the detection of electron-spin resonance, MRFM is also a very promising tool for spatially resolved ferromagnetic resonance force microscopy (FMRFM) and is expected to provide crucial information for future spintronic devices. So far most studies of ferromagnetic materials using MRFM have focused on Yttrium-Iron garnet (YIG) structures with typical lateral dimensions of several tens of micrometers.[3–9] Investigations of materials of more technological interest, in particular metallic ferromagnetic materials, using this technique have been rare.[10–13] The lateral resolution reported both for YIG samples and metallic films is typically of the order of 5 μm (Ref. 13) or larger.

In this paper, we report FMRFM measurements of a 50-nm-thick permalloy film which was patterned into a square array of $d_{\mathrm{disk}}=1.5$ μm diameter disks with a center-to-center distance of 1.8 μm using electron beam lithography; see Fig. 1.

II. EXPERIMENT

In MRFM, a micromagnetic probe tip attached to the end of a compliant cantilever is utilized to define a localized region in which magnetic resonance is excited by monochromatic microwave radiation. In this region, the sum of the external magnetic field $\vec{B}$ and the tip field $\vec{B}_{\mathrm{tip}}(\vec{r})$ matches the resonance condition of the sample. The field gradient produced by the magnetic tip also couples the magnetization $\vec{m}(\vec{r},t)$ of the sample to the cantilever that serves as a high sensitivity, resonant micromechanical force detector. The total force $\vec{F}_{\mathrm{tot}}$ acting on the cantilever is given by[14]

$$\vec{F}_{\mathrm{tot}}(t)=\int_{\mathrm{sample}} dV\vec{F}(\vec{r},t). \tag{1}$$

$\vec{F}(\vec{r},t)$ is the force originating from the volume element located at position $\vec{r}$,

$$\vec{F}(\vec{r},t)=-[\vec{m}(\vec{r},t)\cdot\nabla]\vec{B}_{\mathrm{tip}}(\vec{r}). \tag{2}$$

The microwave field for exciting the magnetic resonance is created using a capacitively coupled bow-tie shaped microstrip resonator with a resonance frequency of about 8 GHz.

In our setup, the cantilever displacement is detected using a fiber optic interferometer [15]; the noise associated with displacement detection is sufficiently low that it can be neglected relative to the thermomechanical displacement noise of the cantilever, even at 4 K. The sample magnetization was modulated at the cantilever resonance frequency f_0, thus exploiting the high-quality factor Q ($\approx 2\times 10^5$) of the mechanical resonator to generate detectable cantilever displacements

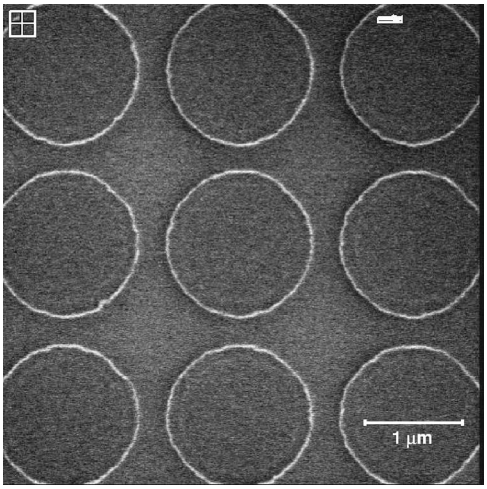

FIG. 1. The sample consisted of a patterned array of 50-nm-thick, 1.5-μm-diam $Ni_{80}Fe_{20}$ disks separated by a center-to-center distance of 1.8 μm.

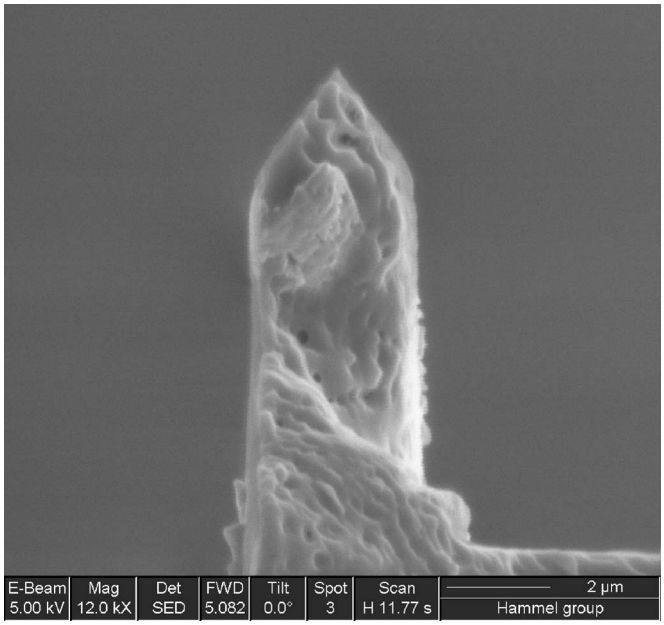

FIG. 2. The SmCo micromagnetic tip used for these experiments was manually attached to the end of a 450-μm-long and 30 -μm-wide lightly boron doped ($\approx 10^{15}$ cm^{-3}) silicon cantilever. The tip was shaped using a focused ion beam mill.

from the small spin forces. This modulation is achieved by modulating the amplitude of the microwave excitation. A commercially available, lightly boron doped ($\approx 10^{15}$ cm^{-3}) Si cantilever[16] was used. A high coercivity SmCo particle is glued to the end of the cantilever and shaped using a focused ion beam; see Fig. 2. The magnetization of the tip is aligned perpendicular to the cantilever beam in an 8 T magnetic field. The coercivity of this tip exceeds 2 T, hence allowing us to apply external magnetic fields antiparallel to the tip moment sufficient to saturate the sample without reversing the tip magnetization. The magnetic moment of the tip $\mu_{\mathrm{tip}} = 1.4 \times 10^{-11}$ J/T was determined by measuring the frequency shift of the cantilever as a function of applied external magnetic field (with the cantilever far from the sample surface). In this case, the frequency shift Δf of the cantilever resonance frequency f_0 is solely due to the torque applied by the homogeneous external magnetic field $B = \mu_0 H$ and is given by[17,18]

$$\frac{\Delta f}{f_0} = \frac{\mu_{\mathrm{tip}} B}{2kL_{\mathrm{eff}}^2}. \tag{3}$$

Here $L_{\mathrm{eff}} = L/1.38 = 360$ μm is the effective length of the cantilever for its first flexural mode in response to an oscillatory torque.[18–20] Experimentally, deviations from a linear field dependence of the frequency shift are small over the entire accessible field range, thus justifying the assumption underlying Eq. (3) of a fixed orientation of the tip magnetization (i.e., a large anisotropy field). The spring constant $k = 0.3$ N/m determined using the method of Sader *et al.*[21,22] is somewhat higher than that estimated by the manufacturer ($k = 0.1-0.2$ N/m) consistent with the observed resonance frequency $f_0 \approx 16.5$ kHz, which is also somewhat higher than the manufacturer's estimate of 10–15 kHz.

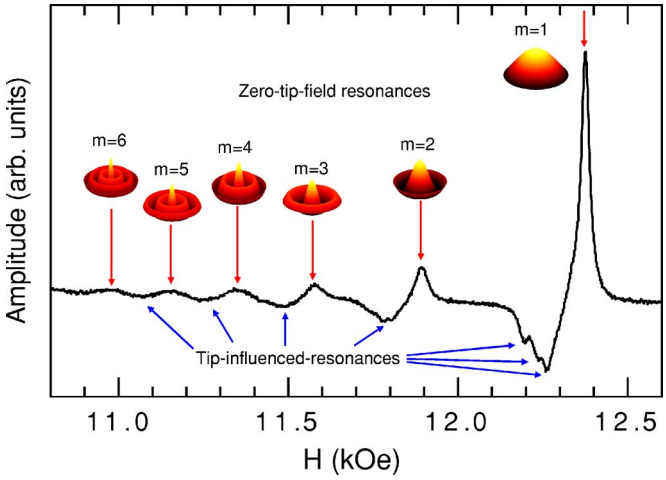

FIG. 3. (Color online) An FMRFM spectrum obtained at a microwave frequency $f_{\mathrm{mw}} = 7.7$ GHz; the amplitude of the microwave excitation was modulated at the cantilever resonance frequency with a depth of 60%. The tip-sample separation was 0.4 μm. The applied magnetic field $\vec{H}$ is aligned along the film normal parallel to the tip magnetization. For each magnetostatic mode, a sketch of the expected lateral variation of transverse moment excited by the microwaves at the particular applied field is also indicated.

III. RESULTS

The results of local FMRFM spectroscopy will be described first, i.e., measurements of the force experienced by the cantilever, hence its oscillation amplitude as a function of applied magnetic field, performed with the magnetic tip above the center of one of the permalloy disks. Using this knowledge of the origin of the different spectral features, the spatially resolved FMRFM images are obtained by laterally scanning the sample surface at fixed magnetic field as described subsequently.

A. Local FMR spectroscopy

A typical FMRFM spectrum is shown in Fig. 3; magnetization in the sample was manipulated using amplitude modulation of the microwave field ($f_{\mathrm{mw}} = 7.7$ GHz) at the cantilever resonance frequency f_0 while sweeping the external magnetic field H, which for all experiments was perpendicular to the plane of the permalloy dots. The frequency f_0 is continuously tracked during field sweep using a PID controller with the phase signal of a lock-in amplifier (typical lock-in time constant 300 ms–1 s) serving as the error signal. The FMRFM spectrum consists of a series of pronounced maxima, each with one or more minima on its low-field side. As will be shown below, the maxima are ferromagnetic resonances of dots far away from the tip for which the tip magnetic field is negligible; we will refer to these as zero-tip-field resonances (ZTFRs). The minima on

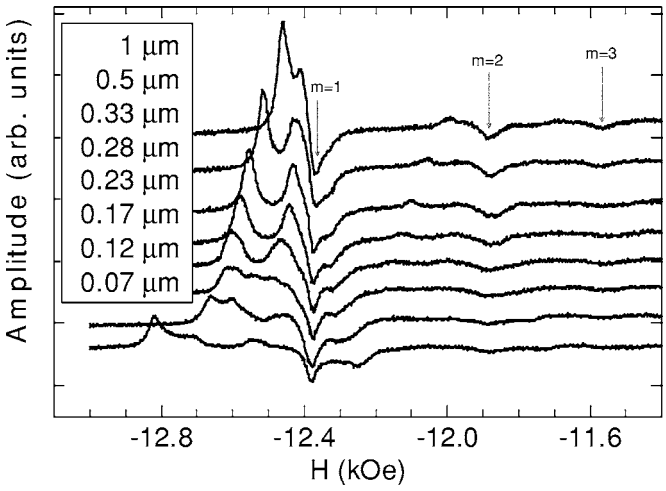

FIG. 4. FMRFM spectra measured at $f_{mw}=7.7$ GHz with 60% amplitude modulation at the cantilever resonance frequency for various tip-sample separations. $\vec{H}$ is aligned along the film normal antiparallel to the tip magnetization. The spectra have been vertically offset for clarity.

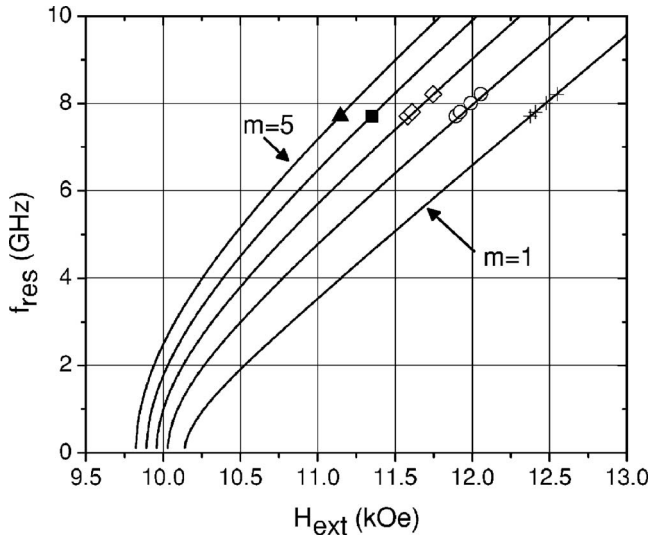

FIG. 5. Comparison of the experimentally determined resonance fields of the modes $m=1,\ldots,5$ for different microwave frequencies (symbols) with theoretical results (solid lines).

the low-field side originate from dots in close proximity to the tip and so are significantly shifted toward smaller fields by the strong tip field. In the following, we will refer to these resonances as tip-influenced resonances (TIRs) to distinguish them from the ZTFRs. We will show that these spectral features provide spatially resolved information about the dynamic magnetic properties of the sample. The fact that ZTFRs are maxima and the TIRs are minima is due to the reversed sign of the tip field gradient for dots far away from the tip and in close proximity to the tip.[14]

The origin of the observed structure in the FMRFM spectrum can be further clarified by recording spectra as a function of the tip-sample separation, as shown in Fig. 4. In this case, the external magnetic field is applied antiparallel to the tip magnetization: this leads to a change in the sign of the force acting on the cantilever. Hence the minima now reflect the ferromagnetic resonances of dots far away from the tip (ZTFR), while the maxima reflect resonances of the dot in close proximity to the tip (TIR). Because the applied field and the sample magnetization are now reversed while the tip magnetization remains unchanged, the TIR of the nearby dot is shifted to more negative field. Reducing the tip-sample distance leads to an increase of the average field experienced by the dot beneath the tip and the TIR shifts away from the ZTFR as the tip approaches and the field position of the ZTFR remains constant, both in agreement with this interpretation.

The ZTFRs are expected to be the same as detected in a conventional FMR experiment. As a consequence of the finite disk diameter, the magnetostatic modes are characterized by discrete in-plane wave vectors $k_{\|}$.[23] Assuming dipolar pinning conditions and zeroth-order Bessel function mode profiles leads to the following condition for the in-plane wave vector: $k_{\|,m}=2\beta_m/d_{\text{disk}}$, where the β_m are the roots of the zeroth-order Bessel function. The mode profiles of the magnetostatic modes excited in the dots resemble modes of a circular membrane [20]; these are sketched in Fig. 3 up to $m=6$. By changing the frequency of the microwave excitation within the bandwidth of our microwave resonator, the dependence of the frequency of the modes on the external magnetic field can be measured, see Fig. 5. For the mode that is uniform across the film thickness (lowest-order mode), the dispersion relation can be expressed in a form similar to the Herring-Kittel dispersion relation[24] for a bulk sample (see Eq. 52 in Ref. 25),

$$\omega_k^2=(\omega_H+\alpha\omega_M k_m^2)[\omega_H+\alpha\omega_M k_m^2+\omega_M f(k_m t)]. \quad (4)$$

Here $\omega_H=\gamma H_i$, where the internal field $H_i=H-N4\pi M_S+H_\perp$, H is the applied field, and M_S is the saturation magnetization of the film, $H_\perp$ is the perpendicular anisotropy field, caused in this particular case by interdot dipolar interactions, γ denotes the gyromagnetic ratio, $\omega_M=4\pi\gamma M_S$, $\alpha=A/2\pi M_S^2$ is the exchange constant, and A is the exchange stiffness constant. The demagnetizing factor N will be inhomogeneous due to the nonellipsoidal dot shape and the internal field will thus be a function of the radial coordinate. Furthermore, since different standing modes in the dot have different radial mode profiles, the effective internal magnetic field will be different for the different modes; see Ref. 23 for details. The term $f(k_m t)=1-[1-\exp(-k_m t)]/k_m t$ accounts for the dipole-dipole interaction for a perpendicularly magnetized individual dot.[26] The values used for the calculation of the first five modes, shown as solid lines in Fig. 5, are as follows: $M_S=828$ emu/cm^3, $\gamma/2\pi=2.96$ MHz/Oe, $A=1.4\times10^{-6}$ erg/cm, and $H_\perp=180$ Oe was estimated for this array geometry using the method described in Ref. 27.

B. Spatially resolved FMRFM

We have shown that the FMRFM spectra contain both local and global information concerning the dynamic properties of the sample in the TIRs and the ZTFRs, respectively. As shown in the preceding section, the ZTFRs are particularly useful to determine the resonance fields of the struc-

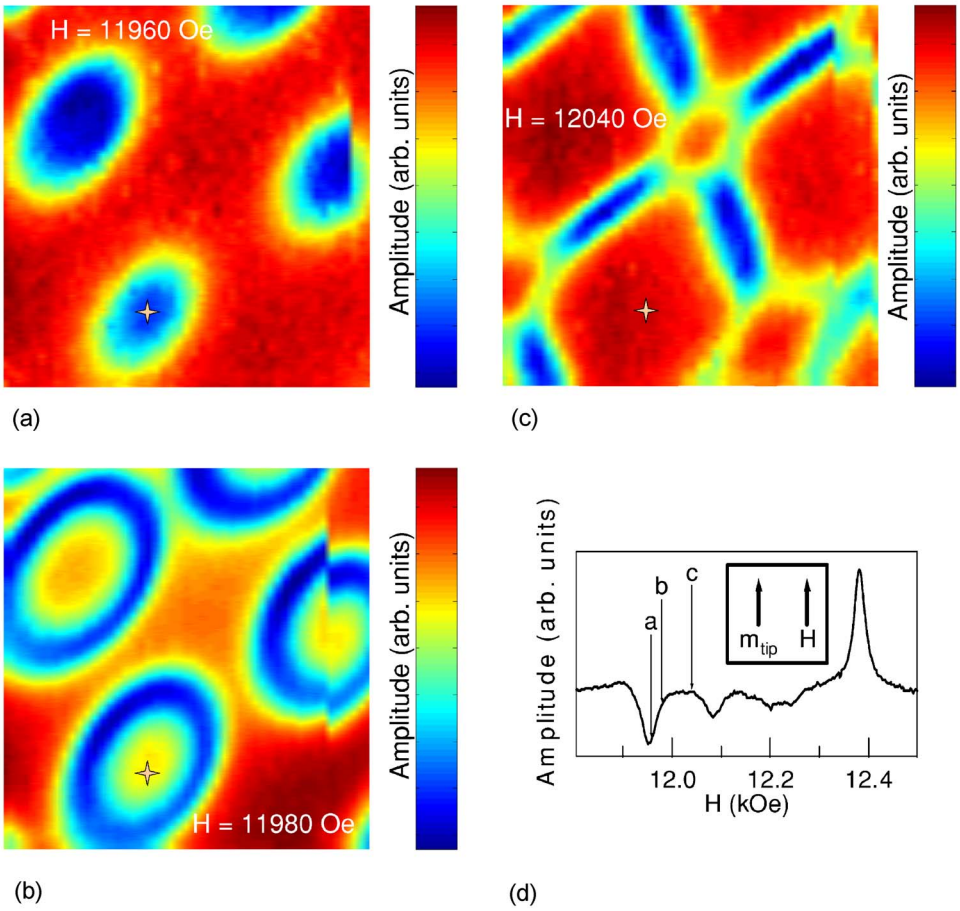

FIG. 6. (Color online) Images obtained at a tip-sample separation of 150 nm and a microwave frequency of f_{mw}=7.7 GHz 60% amplitude modulated at the cantilever frequency are shown. The lower right-hand panel shows the FMRFM spectrum obtained with the tip located over the center of the permalloy dot [indicated by the star in panels (a)–(c)]. Panels (a)–(c) show the cantilever response obtained in lateral scans over an area 2.5 μm$\times$2.5 μm at three external fields: H=11 960, 11 980, and 12 040 Oe. The external magnetic field was aligned parallel to the moment of the tip.

tures and compare them with theoretical predictions. On the other hand, by tuning the field to a TIR located on the low-field side of each ZTFR, spatially resolved images of the dynamic properties responsible for the FMR resonance peak are obtained. In Fig. 6(a), a lateral scan over the sample is shown, with the external field H_{ext}=11 960 G applied parallel to the magnetization of the tip. Selecting this field excites the m=1 resonance of a dot when the tip is located above the center of the dot.

FMRFM imaging in ferromagnetic samples is quite different from paramagnetic samples[3,4] where the resonance frequency is an *entirely local* function of magnetic field. In ferromagnets, the strong exchange and dipolar interactions among spins causes the resonance field to depend on the magnetization of neighboring spins, hence the frequency is sensitive to the magnetization of regions remote from the imaged volume. As recently shown by Urban *et al.*, the inhomogeneous tip field can be taken into account in the calculation of the magnetostatic modes in ferromagnetic samples by performing a series expansion about the modes of the structures[28] that arise in a homogeneous applied field.

To first order, the influence of the tip field on the ferromagnetic resonance in cylindrical dots can then be accounted for by averaging the tip field over the volume of the dot. This is a good approximation as long as the variation of the tip field over the dot is small and thus mixing between the different modes remains negligible. Averaging the tip field over the volume of the dot still requires full knowledge of the spatial variation of the tip magnetic field vector, which we do not have currently. Nevertheless, from symmetry it is clear that the average field experienced by the dot will be largest when the cantilever is placed above the center of the dot and will drop as the cantilever is moved away from the center. By increasing the external magnetic field [see Figs. 6(b) and 6(c)], the total magnetic field experienced by the dot when the tip is located above the center of the dot exceeds the resonance field and thus the magnitude of the force signal is reduced. Moving away from the center of the dot reduces the total magnetic field experienced by the dot and increases the signal magnitude as the peak of the ferromagnetic resonance is approached. The resonant peak is then evident as "resonance rings" whose radii increase with increasing field. At sufficiently high field, rings from neighboring dots will intersect forming crosses, cf. Figs. 6(b) and 6(c). The deviation from cylindrical symmetry observed in the images is caused by the fact that our tip is not precisely circular in cross sec-

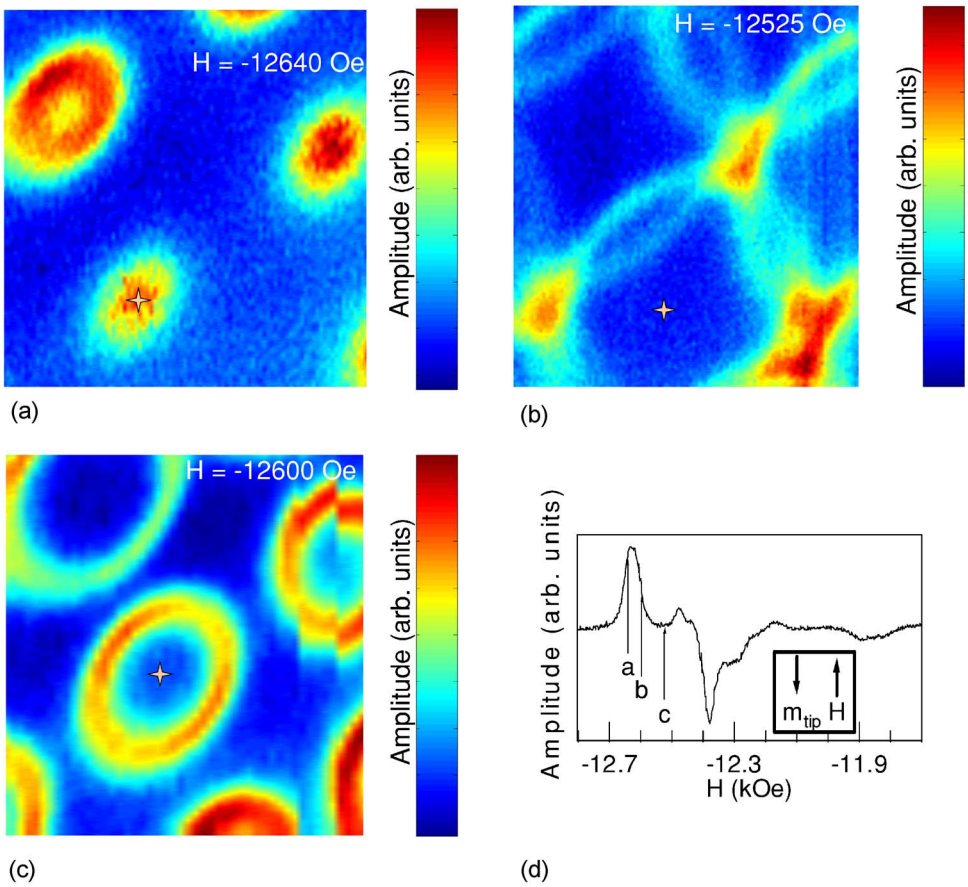

FIG. 7. (Color online) Images obtained at a tip-sample separation of 150 nm and a microwave frequency of f_{mw}=7.7 GHz 60% amplitude modulated at the cantilever frequency are shown. The lower right-hand panel shows the FMRFM spectrum obtained with the tip located over the center of the permalloy dot [indicated by the star in panels (a)–(c)]. Panels (a)–(c) show the cantilever response obtained in lateral scans over an area 2.5 μm×2.5 μm at three external fields: H=−12 640, −12 600, and −12 525 Oe. The external magnetic field was aligned antiparallel to the moment of the tip.

tion and its tip is slightly elongated along the diagonal of the images. The tip is also slightly tilted with respect to the surface normal of the film (10°–15°).

By applying the external field antiparallel to the tip, it is possible to produce a region of reduced field just beneath the tip; this is possible because the SmCo tip has a coercivity much larger than the fields applied (cf. Fig. 4). The tip field resonance features of the spectrum again can be used to obtain spatially resolved images of the ferromagnetic resonance of the dots, as is shown in Figs. 7(a)–7(c). The contrast in the images is reversed as compared to those of Figs. 6(a)–6(c) because the sign of the force is opposite in the two cases.

The extension of local FMR imaging to continuous films would open up a new approach to local studies of the dynamic properties of a continuous film sample. This would allow, e.g., detection of imperfections or spatial variation of dynamic properties in wedge-shaped samples, a capability not available using conventional FMR techniques. The ability to apply large tip fields, both positive and negative, will provide a useful degree of freedom in pursuing this objective.

IV. CONCLUSIONS

Magnetic resonance force microscopy has been used to detect the ferromagnetic resonance of micron-sized permalloy disks. Local spectroscopy at various tip-sample distances enables the separation of spectral features associated with the global and local dynamic properties of the sample. The global properties are in good agreement with theoretical predictions and previous experimental investigations using conventional FMR or Brillouin light scattering techniques. The quantized magnetostatic modes of the permalloy dots are clearly visible in the spectra. The spectral features associated with resonances in close proximity to the magnetic tip provide two-dimensional images of the sample in which individual dots are clearly resolved. By using a hard magnetic tip, we are able to image with the tip magnetization aligned either parallel or antiparallel to the external field. Further improvement of the spatial resolution is possible by shaping the tip into a finer needle. As this should further increase the field gradient produced by the tip, this would also further increase the sensitivity of the magnetic resonance force microscope.

*Electronic address: tmewes@ua.edu
†Electronic address: hammel@mps.ohio-state.edu

[1] J. A. Sidles, Appl. Phys. Lett. **58**, 2854 (1991).
[2] D. Rugar, R. Budakian, H. J. Mamin, and B. W. Chui, Nature (London) **430**, 329 (2004).
[3] Z. Zhang, P. C. Hammel, and P. E. Wigen, Appl. Phys. Lett. **68**, 2005 (1996).
[4] K. Wago, D. Botkin, C. S. Yannoni, and D. Rugar, Appl. Phys. Lett. **72**, 2757 (1998).
[5] M. M. Midzor, P. E. Wigen, D. Pelekhov, W. Chen, P. C. Hammel, and M. L. Roukes, J. Appl. Phys. **87**, 6493 (2000).
[6] V. Charbois, V. V. Naletov, J. B. Youssef, and O. Klein, Appl. Phys. Lett. **80**, 4795 (2002).
[7] V. Charbois, V. V. Naletov, J. B. Youssef, and O. Klein, J. Appl. Phys. **91**, 7337 (2002).
[8] V. V. Naletov, V. Charbois, O. Klein, and C. Fermon, Appl. Phys. Lett. **83**, 3132 (2003).
[9] O. Klein, V. Charbois, V. V. Naletov, and C. Fermon, Phys. Rev. B **67**, 220407 (2003).
[10] B. J. Suh, P. C. Hammel, Z. Zhang, M. M. Midzor, M. L. Roukes, and J. R. Childress, J. Vac. Sci. Technol. B **16**, 2275 (1998).
[11] Z. Zhang, P. C. Hammel, M. Midzor, M. L. Roukes, and J. R. Childress, Appl. Phys. Lett. **73**, 2036 (1998).
[12] J. Moreland, M. Lohndorf, P. Kabos, and R. D. McMichael, Rev. Sci. Instrum. **71**, 3099 (2000).
[13] A. Volodin, D. Buntinx, S. Brems, and C. V. Haesendonck, Appl. Phys. Lett. **85**, 5935 (2004).
[14] A. Suter, D. Pelekhov, M. Roukes, and P. Hammel, J. Magn. Reson. **154**, 210 (2002).
[15] D. Rugar, H. J. Mamin, and P. Guethner, Appl. Phys. Lett. **55**, 2588 (1989).
[16] *Mpp-32100-50 light contact mode silicon probe*, Veeco Metrology LLC.
[17] Z. Zhang and P. C. Hammel, Solid State Nucl. Magn. Reson. **11**, 65 (1999).
[18] B. C. Stipe, H. J. Mamin, T. D. Stowe, T. W. Kenny, and D. Rugar, Phys. Rev. Lett. **86**, 2874 (2001).
[19] J. A. Sidles, J. L. Garbini, K. J. Bruland, D. Rugar, O. Zuger, S. Hoen, and C. S. Yannoni, Rev. Mod. Phys. **67**, 249 (1995).
[20] P. Morse and K. Ingard, *Theoretical Acoustics* (McGraw-Hill Book Company, New York, 1968).
[21] J. E. Sader, J. Appl. Phys. **84**, 64 (1998).
[22] J. E. Sader, J. W. M. Chon, and P. Mulvaney, Rev. Sci. Instrum. **70**, 3967 (1999).
[23] G. N. Kakazei, P. E. Wigen, K. Y. Guslienko, V. Novosad, A. N. Slavin, V. O. Golub, N. A. Lesnik, and Y. Otani, Appl. Phys. Lett. **85**, 443 (2004).
[24] C. Herring and C. Kittel, Phys. Rev. **81**, 869 (1951).
[25] B. Kalinikos and A. Slavin, J. Phys. C **19**, 7013 (1986).
[26] B. A. Kalinikos, IEE Proc., Part H: Microwaves, Opt. Antennas **127**, 4 (1980).
[27] G. N. Kakazei, Y. Pogorelov, M. D. Costa, T. Mewes, P. E. Wigen, P. C. Hammel, V. Golub, T. Okuno, and V. Novosad, Phys. Rev. B **74**, 060406(R) (2006).
[28] R. Urban, A. Putilin, P. E. Wigen, S.-H. Liou, M. C. Cross, P. C. Hammel, and M. L. Roukes, Phys. Rev. B **73**, 212410 (2006).